

Electronic supplementary information

**Improving the performance of biomass-based electrocatalysts
by means of hot pressing**

Tianhao Huang, ^a Wendu Zhang, ^{*a,b} Weiqi Liu, ^a Shilin Wei, ^a Wujun Geng, ^a Xue Xia
^a and Lang Xu ^{*a}

** Corresponding authors*

*^a MOE Key Laboratory of Coal Processing and Efficient Utilization, School of Chemical Engineering
and Technology, China University of Mining and Technology, 1 Daxue Road, Xuzhou, Jiangsu,
221116, China*

Email: lang.xu@cumt.edu.cn (L. Xu)

*^b School of Grain, Food and Medical Products, Jiangsu Vocational College of Finance and
Economics, 8 East Meicheng Road, Huai'an, Jiangsu, 223003, China*

E-mail: jscjzwd@163.com (W. Zhang)

Characterization techniques

Scanning electron microscopy (SEM) images were taken on a FEI Quanta FEG 250 field-emission scanning electron microscope, equipped with an energy dispersive X-ray (EDX) microanalysis. N₂ (at 77 K) adsorption-desorption isotherm measurements were conducted using a Quantachrome Autosorb-iQ physisorption analyzer. Macropore width distributions were acquired on a Micromeritics AutoPore IV 9500 mercury intrusion porosimeter (MIP). X-ray photoelectron spectroscopy (XPS) measurements were carried out on a Thermo Scientific ESCALAB 250Xi X-ray photoelectron spectrometer using the Al K α line (1486.6 eV). Raman spectra were obtained on a Bruker Senterra confocal Raman spectrometer using a laser with the wavelength of 532 nm.

Electrochemical methods

Electrode preparations

All electrochemical experiments in this work were performed in a three-electrode configuration, using an Ivium electrochemical workstation (IviumStat.h, Ivium Technologies). For the three electrodes, a rotating disk or ring (Pt)-disk glassy carbon working electrode was used in conjunction with an electrode rotator (AFMSRCE, Pine Research), a graphite rod was employed as a counter electrode, and an Ag/AgCl electrode held in a Luggin tube containing 3.5 M KCl was used as a reference electrode. The potentials (recorded versus an Ag/AgCl electrode) were converted to the reversible hydrogen electrode (RHE) scale using $E_{\text{RHE}} = E_{\text{Ag/AgCl}} + 0.205 \text{ V} + 0.059 \cdot \text{pH}$ (at 25 °C). The rotating disk (or ring-disk) electrode was first polished by an aqueous Al₂O₃ slurry on a piece of chamois cloth and then rinsed thoroughly using ultrapure water. To prepare a catalyst ink for the working electrode, 2.0 mg of a biomass-based electrocatalyst or 1.0 mg of the standard electrocatalyst 20wt% Pt/C was uniformly mixed with 170 μL of ultrapure water, 70 μL of isopropanol, and 10 μL of 5 wt% Nafion

perfluorinated resin solution by means of ultrasonic wave. The catalyst ink was pipetted onto the freshly polished rotating disk (or ring-disk) electrode. The catalyst loading on the working electrode is 0.4 mg cm^{-2} for a biomass-based electrocatalyst or 0.2 mg cm^{-2} for Pt/C.

Electrocatalytic measurements

Electrocatalytic reduction of O_2 is the object of study. Electrolytes used in the electrocatalytic measurements include 0.1 M KOH and 0.5 M H_2SO_4 . A constant gas flows of N_2 or O_2 was first flushed into the electrolyte solution to remove possible gas impurities prior to the electrochemical experiments and then through the cell headspace during the measurements. In this work, cyclic voltammetry experiments were conducted without rotation, whereas linear sweep voltammetry and rotating ring-disk electrode measurements were performed with a rotation rate of 1600 rpm. To deal with linear sweep voltammograms, currents recorded in the N_2 -saturated electrolyte were subtracted from those in the O_2 -saturated one in order to remove capacitive currents of carbonaceous catalysts. By means of the rotating ring-disk electrode technique, electron-transfer numbers and percentage yields of peroxide were measured by the equations

$$n = 4 \frac{i_D}{i_D + \frac{i_R}{N}}$$

$$\text{peroxide}\% = 200 \frac{\frac{i_R}{N}}{i_D + \frac{i_R}{N}}$$

where n is the electron-transfer number, i_D is the disk current, i_R is the ring current, *peroxide%* is the percentage yield of peroxide, and N is the ring collection efficiency of Pt ring (0.37). Current stability was measured using chronoamperometry at a fixed electrode potential, which was the half-wave potential of HPBE (0.84 V in the alkaline electrolyte and 0.68 V in the acidic one), at a rotation rate

of 400 rpm. Electrochemical impedance spectroscopy experiments were carried out at an amplitude of 10 mV in a frequency range $10^5 \sim 10^{-2}$ Hz.

The mass-transport corrected Tafel analysis was conducted according to the paper by Compton et al.,¹ using the mass-transport corrected transfer coefficient α' :

$$\alpha' = \frac{RT}{F} \frac{d \ln \left| \frac{1}{i} - \frac{1}{i_{lim}} \right|}{dE}$$

where R is the gas constant ($8.314 \text{ J mol}^{-1} \text{ K}^{-1}$), T is the temperature in K, F is the Faraday constant (96485 C mol^{-1}), E is the potential of the working electrode, i is the current, and i_{lim} is the mass-transport limiting current.

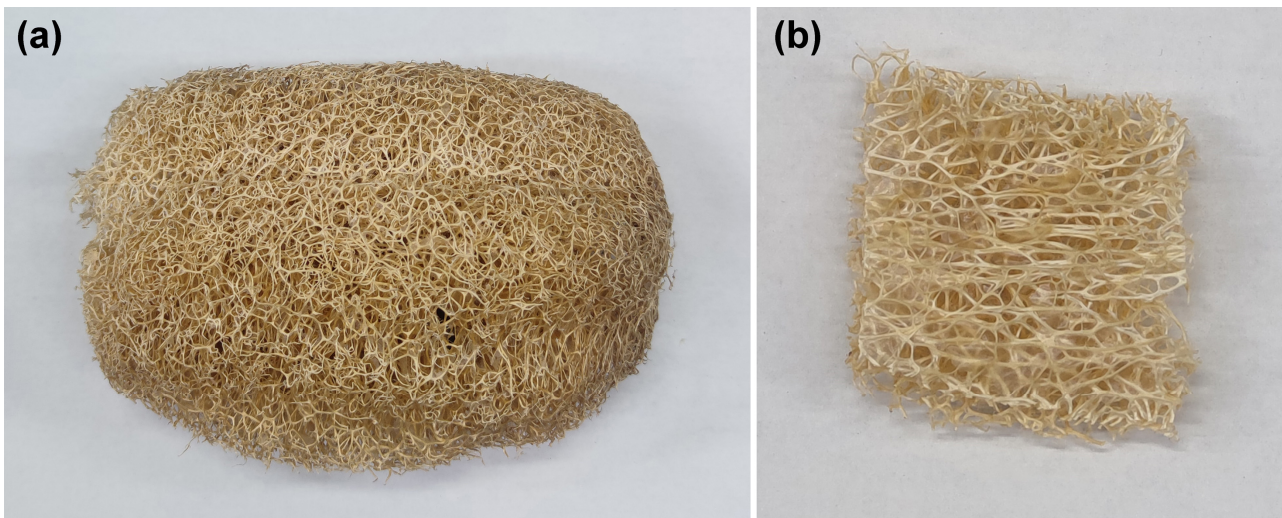


Fig. S1 Photographic images of a fibrous interior of a mature fruit of raw sponge gourd (*Luffa aegytiaca*) (a) and a small piece of this fibrous interior (b).

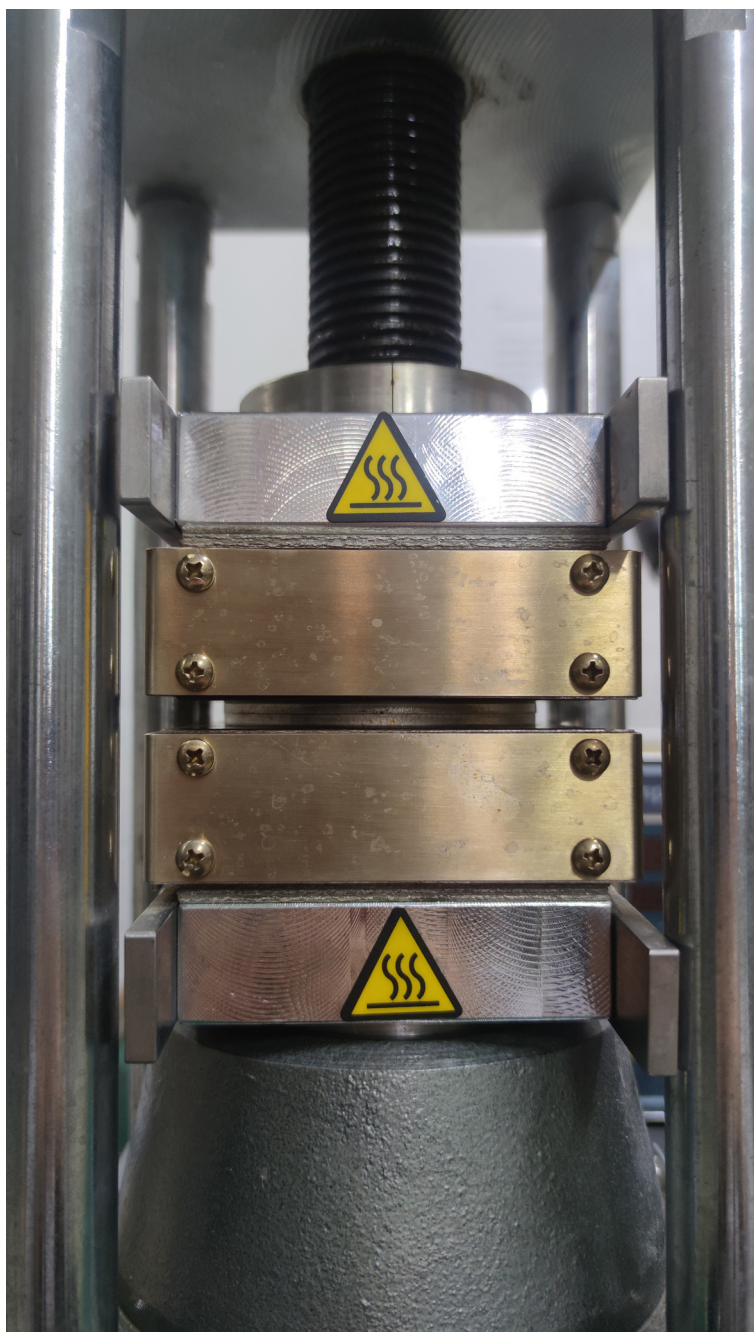


Fig. S2 A photographic image of a hot press used in this work.

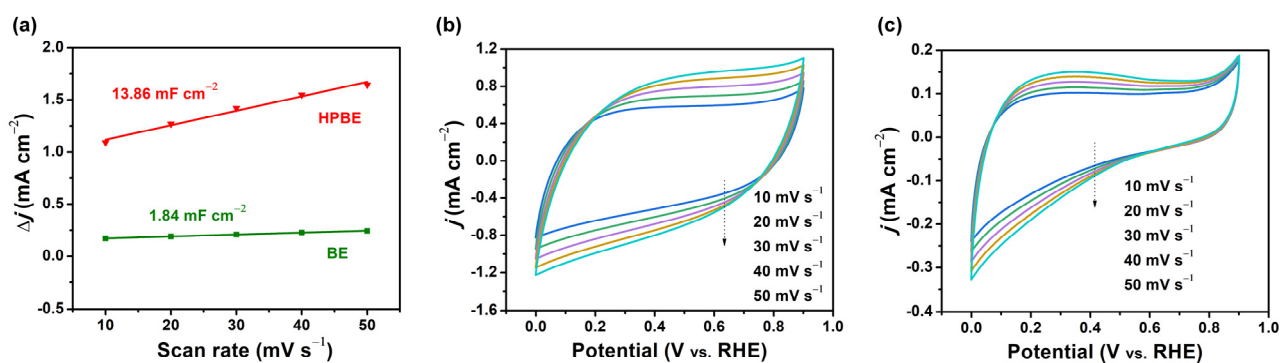


Fig. S3 Charging current density differences plotted against scan rates for HPBE and BE (a). Cyclic voltammograms of HPBE (b) and BE (c) at different scan rates in 0.1 M KOH.

According to the literature,^{2,3} if a catalyst has a larger ECSA value, then it should have more active sites, and it is known that the larger the specific capacitance of a material, the larger the ECSA. As shown in Fig. S3, the double-layer capacitance of HPBE is 13.86 mF cm^{-2} , which is much larger than that of BE (1.84 mF cm^{-2}), suggesting that the former with the increased N content has a far larger ECSA and therefore much more active sites. In this sense, the hot-pressing method favours the doping of numerous nitrogen atoms into the carbon matrices and therefore the formation of abundant active sites.

References

- [1] D. Li, C. Lin, C. Batchelor-McAuley, L. Chen, R. G. Compton, *J. Electroanal. Chem.*, 2018, **826**, 117-124.
- [2] W. Liu, J. Qi, P. Bai, W. Zhang, L. Xu, *Appl. Catal. B: Environ.*, 2020, **272**, 118974.
- [3] W. Liu, S. Wei, P. Bai, C. Yang, L. Xu, *Appl. Catal. B: Environ.*, 2021, **299**, 120661.